

# Simulation of exercise-dependent difference in metabolism with a mathematical model for analyses of measurements using near-infrared spectroscopy

K. J. Kek, T. Miyakawa, S. Yoneyama, N. Kudo, *Member, IEEE*, and K. Yamamoto, *Member, IEEE*

**Abstract** — Near-infrared spectroscopy (NIRS) is a useful technique for noninvasive measurement of muscle oxygenation. However, analyses of the dynamic changes in muscle metabolism based only on experimental observations of NIRS are difficult. Therefore, we constructed a mathematical model of muscle metabolism, comprising of the ATP synthesizing systems and O<sub>2</sub> diffusion system, to identify the mechanisms responsible for those observations. A customized NIRS instrument was used to measure the changes in muscle oxygenation of the forearm flexor muscles during intermittent and continuous isometric flexion exercises when healthy male subjects participated in exercises tests. The exercise-dependent difference in changes could be distinguished and the simulated results agreed well with that measured experimentally. Although the contraction intensity for both exercises was identical, the magnitude of energy needed to perform the respective exercises was different. This difference was reflected by the changes in the ATP synthesizing systems, in which the energy needed during the latter-half of continuous exercise was mostly supplied by anaerobic system, whereas that during intermittent exercise was supplied by the aerobic and anaerobic systems that operated synergistically. From the results, we conclude that the model could be a useful tool for the elucidation of the relationship between experimental observations of NIRS and muscle metabolism.

## I. INTRODUCTION

Near-infrared spectroscopy (NIRS) is a useful technique for noninvasive measurement of muscle oxygenation. We have shown that the synergistic function of the quadriceps muscle during two different isometric knee extension exercises could be distinguished using NIRS [1]. However, the changes in muscle oxygenation during exercise could be affected by different factors of the complex metabolic system: the synergistic function of the aerobic and anaerobic metabolic systems, the changes in O<sub>2</sub> concentration gradient between the blood vessels and muscle cells that affects the O<sub>2</sub> diffusion rate, and the relative contribution of hemoglobin and myoglobin to the NIRS signals. Consequently, analyses of the changes in muscle metabolism based only on experimental observations of NIRS are difficult.

In this study, we attempt to address the problem by constructing a mathematical model of muscle metabolism to identify the primary mechanisms responsible for experimental observations of NIRS and to elucidate its relationship with muscle metabolism. In recent years, various models have been constructed for the detailed study of different metabolic pathways. For example, Paolo et al. [2] reported a model that fits the experimental results of phosphocreatine

(PCr) changes during ischemia and exercise well. In comparison, Korzeniewski et al. [3] constructed a model that predicts the difference in activation of aerobic metabolism during low and high work intensities with good accuracy. These promising results show that the models could be applied to investigate physiological events that are difficult to be directly captured by conventional instruments. However, owing to their high complexity, interpretation of the essential elements that contributes to the characteristic changes in the metabolic pathways is difficult. In addition, the mechanism of O<sub>2</sub> transport from blood to tissue, an important element of aerobic metabolism, is not considered in these works.

Therefore, we aimed to construct a simple model that incorporates both the aerobic and anaerobic metabolic systems and the O<sub>2</sub> transport mechanism from blood to tissue. We used the constructed model to reproduce the temporal responses of O<sub>2</sub> concentration and O<sub>2</sub> consumption rate ( $\dot{V}O_2$ ) that was obtained from NIRS experimental results. In addition, we evaluated the synergistic function of the aerobic and anaerobic metabolic systems and O<sub>2</sub> transport mechanism during different exercise protocols using the simulation results.

## II. MATERIALS AND METHODS

### A. *In vivo measurement using NIRS*

Five healthy male adults participated in exercise tests. Their mean (SD) age, weight and height were 23.6 (1.1) years, 62.4 (7.6) kg and 172.2 (5.4) cm, respectively. We obtained informed consent for participation in the study from all subjects prior to the measurements.

The subjects performed exercise tests at 70% maximum voluntary contraction (%MVC) with the following protocols: (1) 3-s isometric contraction (repeated 10 times)/1-s relaxation (repeated 9 times) for a total duration of 39 s, and (2) 39-s continuous isometric contraction. Measurements were made on the flexor muscles of the forearm using a spatially resolved NIRS instrument [1].

Arterial occlusion was performed on the forearm with a sphygmomanometer (280 mmHg) to interrupt the O<sub>2</sub> supply to the measurement site. Blasi showed that the initial rate of oxy-hemoglobin ( $HbO_2(t)$ ) deoxygenation during arterial occlusion reflects the direct measurement of local  $\dot{V}O_2$  [4]. Therefore, we performed arterial occlusion for 30 s from 120 s before the start of exercise to calculate the resting  $\dot{V}O_2$ , and for 5 to 15 s from 5, 20, 40, and 70 s after the end of exercise, respectively, to calculate the recovery  $\dot{V}O_2$ .

During exercise, contraction at relatively high intensity ( $\geq 70\%$  MVC) resulted in spontaneous occlusion of blood flow to the muscle due to the elevated intramuscular pressure. The rate of  $HbO_2(t)$  deoxygenation during continuous contraction, where blood flow is restricted, is a good indicator of exercising local  $\dot{V}O_2$  [5].

---

The authors are with the Graduate School of Information Science and Technology, Hokkaido University, 060-0814 Japan. (Phone: +81-11-706-6777; fax: +81-11-706-7802; e-mail: {kek, miyakawa, yone, kudo, yamamoto}@bme.ist.hokudai.ac.jp). This study was supported in part by a research fellowship awarded to K. J. Kek and by a Grant-in-Aid for Scientific Research from the Japan Society for the Promotion of Science.

From the above, we calculated the local  $\dot{V}_{O_2}$  during different phases (rest, exercise and recovery) from the slope of decreasing rate of  $HbO_2(t)$  by linear regression. The concentration of oxy-myoglobin ( $MbO_2(t)$ ) is included in the calculation because its absorption spectrum is almost identical with that of  $HbO_2(t)$ . As a result, they cannot be distinguished using NIRS.

### B. Simulation with a model of muscle metabolism

Fig. 1 shows the schematic of the two-system, two-compartment model. The model is composed of two primary systems: (a) the adenosine triphosphate (ATP) synthesizing system that consists of the aerobic and anaerobic compartments, and (b) the oxygen diffusion system that consisting of the blood and tissue compartments. For modeling purposes, the following assumptions hold:

- 1) The model is composed of control systems that function as ATP buffer.
- 2) Adenosine diphosphate (ADP) is the control input since ADP is the substrate for ATP synthesis.
- 3) Only first or second-order kinetic equations are used. The kinetics of enzyme are ignored.

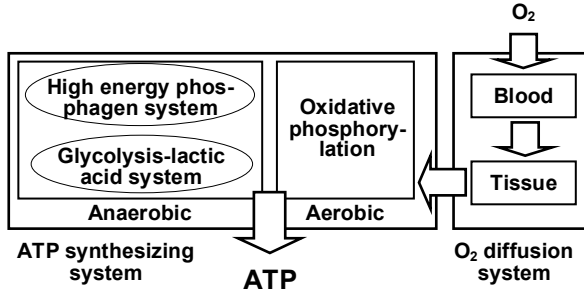


Fig. 1. Schematic of the metabolic model. See text for details.

From the above, we obtained the following equation that represents the two-compartment ATP synthesizing system for the model,

$$\dot{ADP}(t) = \dot{q}_{total} - \dot{q}_{ATP,PCr} - \dot{q}_{ATP,GI} - \dot{q}_{ATP,O_2}, \quad (1)$$

where the single dot represents the time ( $t$ ) derivative,  $\dot{q}_{total} = (\chi w + 1)q_o + \sigma Cr(t)ATP(t)$  represents the total ATP consumption rate (ATP demand) with respect to basal metabolism  $q_o$  and an adjustable coefficient  $\chi$ , represents the ATP consumption rate that is equivalent to the corresponding exercise intensity  $w$  during *in vivo* measurements.  $Cr(t)$  and  $ATP(t)$ , described by  $(Cr_o + PCr_o - PCr(t))$  and  $(ATP_o + ADP_o - ADP(t))$ , respectively, represent the change in creatine (Cr) and ATP concentrations during PCr resynthesis.  $Cr_o$ ,  $PCr_o$ ,  $ATP_o$ , and  $ADP_o$  represent the initial concentration of Cr, PCr, ATP, and ADP, respectively. The ATP synthesis rate, given in (1), consists of three components and is proportional to  $ADP(t)$ :

$$\dot{q}_{ATP,PCr} = \gamma PCr(t)ADP(t), \quad (2)$$

$$\dot{q}_{ATP,GI} = \delta GI(t)ADP(t), \text{ and} \quad (3)$$

$$\dot{q}_{ATP,O_2} = \zeta ADP(t) \left\{ \frac{P_t(t) - \alpha}{P_t(t) - \alpha + \beta} \right\}, \quad (4)$$

where  $\dot{q}_{ATP,PCr}$  and  $\dot{q}_{ATP,GI}$  are the rates of PCr breakdown and anaerobic glycolysis, respectively, during anaerobic metabolism.  $\dot{q}_{ATP,O_2}$  is the rate of oxidative phosphorylation

during aerobic metabolism.  $PCr(t)$ ,  $GI(t)$  and  $P_t(t)$  represent the concentrations of PCr, the concentrations of blood glucose and muscle glycogen, and the partial pressure of  $O_2$  of the tissue compartment, respectively. The constants  $\gamma$ ,  $\delta$  and  $\zeta$  describe the product of the unit conversion coefficients (between ATP synthesis/consumption and reactant consumption/synthesis) and the rate constants of the respective reactions.  $\alpha$  and  $\beta$  are arbitrary constants that determine the transition from aerobic to anaerobic metabolism that will occur during severe hypoxia

The diffusion of oxygen from capillaries (blood) into the muscle cells (tissue) is represented by two compartments:

$$\dot{C}_v = \dot{Q}(C_a - C_v) - G(P_v(t) - P_t(t)), \quad (5)$$

$$\dot{C}_t = G(P_v(t) - P_t(t)) - \dot{q}_{ATP,O_2}, \quad (6)$$

where  $\dot{C}_v$  and  $\dot{C}_t$  represent the time derivative of the  $O_2$  concentration in the venous blood and tissue compartments, respectively.  $C_a$  represents the  $O_2$  concentration in the arterial blood compartment.  $G$  is a constant that determines the rate of  $O_2$  diffusion between the venous and the tissue compartments.  $P_v(t)$  represents the partial pressure of  $O_2$  of the venous compartment and  $\dot{Q}$  is a  $P_t(t)$  dependent variable that is used to simulate the changes in blood flow. We solved (5) and (6) by partial differentiation with the equations derived from the dissociation curve of hemoglobin and myoglobin, respectively. The differential equations were numerically solved with Mathematica<sup>®</sup> version 4.0. The main parameters and constants, referred from reported values, were summarized in Table 1.

## III. RESULTS

### A. Comparison of experimental and simulated $\dot{V}_{O_2}$

As shown in Fig. 2(a), after the peak  $\dot{V}_{O_2}$  (about 8–12 times greater than resting  $\dot{V}_{O_2}$ ) was reached 10–15 s after the onset of exercise,  $\dot{V}_{O_2}$  of both protocols decreased and reached a plateau at about 20 s. The decrement of  $\dot{V}_{O_2}$  of protocol 2 was greater than that of protocol 1 and was maintained at approximately zero at the latter-half of the exercise, indicating that the energy needed to maintain the muscle contraction was mainly supplied by anaerobic metabolism. During recovery,  $\dot{V}_{O_2}$  of both exercises was high (about 7–12 times greater than resting  $\dot{V}_{O_2}$ ) due to significant excess post exercise oxygen consumption ( $O_2$  debt). The maximum  $\dot{V}_{O_2}$  was reached at the second or third post-exercise arterial occlusion.

For simulation of  $\dot{V}_{O_2}$  using the model, we varied  $\dot{Q}$  according to different situations, such as occlusion, exercise and recovery to simulate the corresponding changes in  $HbO_2(t)$  during the exercise tests described in section II.A. We then calculated  $\dot{V}_{O_2}$  from the slope of decreasing rate of the simulated  $HbO_2(t)$  by linear regression. The characteristic changes in temporal response of  $\dot{V}_{O_2}$  were sufficiently reproduced in Fig 2(b). The changes are probably due to the difference in the rate and amount of energy that was produced and consumed in response to different exercise.

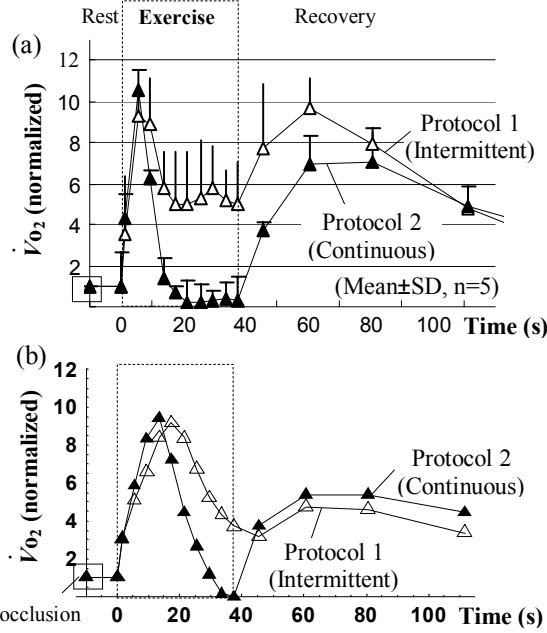


Fig. 2. (a)  $\dot{V}_{O_2}$  calculated from NIRS experimental values, and (b) simulated  $\dot{V}_{O_2}$  (Normalized using resting  $\dot{V}_{O_2}$ )

### B. Synergistic function of ATP synthesizing and $O_2$ diffusion systems in response to different exercises

As shown in Fig. 3(a),  $P_i(t)$  decreased immediately after the start of intermittent exercise due to the increase in  $O_2$  demand. This is evident from Fig. 3(b), where the insufficient increase in the ATP synthesis rate by aerobic metabolism was met by a concomitant increase in that by anaerobic metabolism. As exercise progressed,  $P_i(t)$  decreased more rapidly than  $P_v(t)$ , indicating that  $O_2$  consumption in the tissue compartment occurred at a more rapid rate than  $O_2$  supply from the blood compartment. Due to the enhanced  $O_2$  concentration gradient between the blood and the tissue compartments,  $O_2$  diffusion rate increased to meet the increase in  $O_2$  demand.  $P_i(t)$  and  $P_v(t)$  reached a plateau of about 1 mmHg and 15 mmHg approximately 20 s and 30 s, respectively, after the start of exercise. When the plateau is reached, ATP synthesis by aerobic metabolism decreased whereas that by anaerobic metabolism increased to complement the ATP production that was needed to sustain the remaining exercise.

In contrast,  $P_i(t)$  decreased more rapidly during continuous exercise, indicating that  $\dot{V}_{O_2}$  during continuous exercise was much higher than that during intermittent exercise (Fig. 3(c)). Consequently,  $P_i(t)$  reached the plateau of about zero much faster, approximately at 15 s after the start of exercise, whereas  $P_v(t)$  reached a plateau of the same level approximately at 25 s. When the plateau of  $P_i(t)$  was reached, the ATP synthesis rate by aerobic metabolism decreased whereas that by anaerobic metabolism increased (Fig. 3(d)). Contrary to that during intermittent exercise, aerobic metabolism cannot produce the ATP needed when both  $P_i(t)$  and  $P_v(t)$  falls approximately to zero. Consequently, the en-

ergy needed to sustain the remaining exercise was supplied only by anaerobic metabolism.

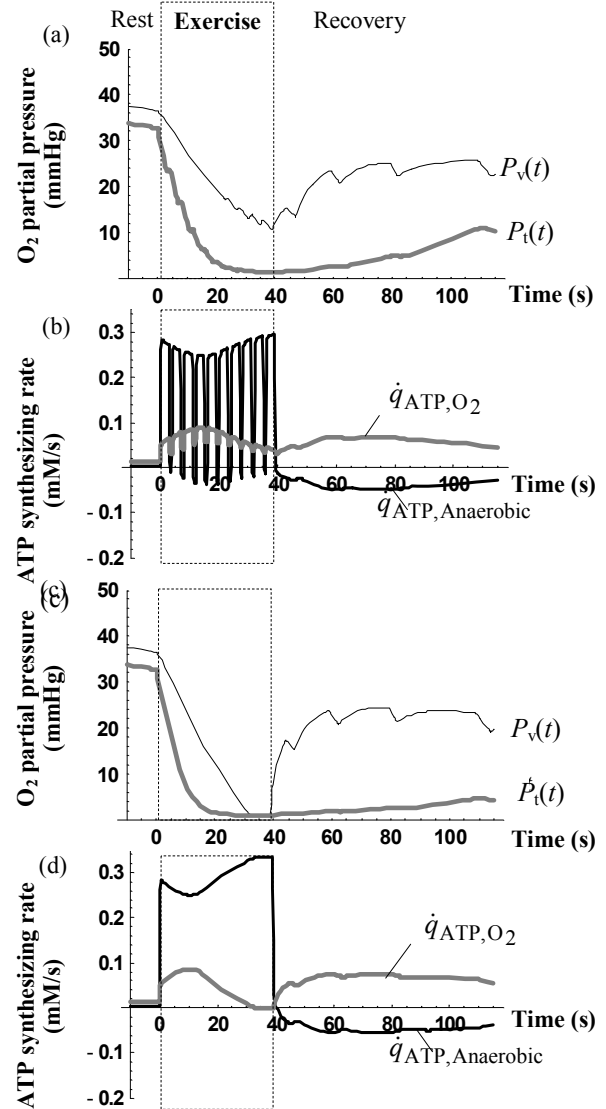


Fig. 3. Simulated temporal changes in  $P_v(t)$  and  $P_i(t)$ , as well as those in aerobic and anaerobic ATP syntheses during exercise in protocol 1 (intermittent exercise), (a) and (b), and in protocol 2 (continuous exercise), (c) and (d). ( $\dot{q}_{ATP,Anaerobic} = \dot{q}_{ATP,PCr} + \dot{q}_{ATP,GI}$ )

After the end of exercise, the ATP synthesis rate by aerobic metabolism increased for about the first 20 s, the rate of continuous exercise being faster due to higher oxygen debt. During the same period, the ATP synthesis rate by anaerobic metabolism falls to negative since the ATP consumption rate for PCr resynthesis was more rapid than the ATP synthesis rate by anaerobic metabolism (Fig. 3(b) and (d)). The slow recovery of  $P_i(t)$  to resting level during recovery probably reflected the time needed for myoglobin reoxygenation in tissue.

### IV. DISCUSSION

Fig. 2(a) shows that the maximum recovery  $\dot{V}_{O_2}$  was not reached immediately after the end of exercise. During this

metabolic state,  $\dot{V}_{O_2}$  could still be extremely low. The slow recovery of  $P_t(t)$ , as shown in Fig. 3(a) and 3(c), indicated that the availability of  $O_2$  after the end of exercise is one of the main regulating factors of  $\dot{V}_{O_2}$  [6].

The simulation results show that although the instantaneous ATP demand for both exercise protocols was set to be identical, the aerobic and anaerobic ATP synthesizing systems and  $O_2$  diffusion system operated synergistically according to different exercise protocols. In addition, the transition from aerobic to anaerobic metabolism probably occurs when  $P_t(t)$  falls approximately to zero, i.e. severely hypoxic condition, since in such situation most of the bounded  $O_2$  of both hemoglobin and myoglobin are released and the oxidative phosphorylation process is ceased.

The strength of our approach is that only a minimum number of essential mechanisms were integrated into the model. Our model is significant in which several equations offer a good macroscopic view of the exercise-dependent difference in the metabolic changes in muscle.

In contrast, the limitation of our simplified modeling of metabolic changes in muscle is that the details of some mechanism that involved enzyme cannot be simulated accurately. For example, we did not include the Michaelis-Menten kinetics for enzymes of relevant physiological mechanisms, such as the creatine kinase reaction and glycolysis in the model. Therefore, the simulation results reported here would likely be changed if these mechanisms were considered in the model. In addition, we also assumed that ADP is the control input for all systems, whereas various substrates function as the control input in the actual metabolic system. Moreover, we need to establish a more quantitative method of determining the relationship between  $\chi$  and %MVC. The inclusion of rate constants that describe each specific phase of the exercise is also probably necessary [2, 14].

## V. CONCLUSION

The results show that the experimentally calculated  $\dot{V}_{O_2}$  was reproduced by simulation in spite of the highly simplified properties of these equations and the low number of mechanism modeled. In addition, the resulting final picture

sufficiently accounts for the synergistic features of the ATP synthesizing systems and  $O_2$  diffusion system. The results also show the close relationship between  $\dot{V}_{O_2}$  and partial pressure of  $O_2$  of the blood and tissue compartments. We conclude that the preliminary results lay the foundation of a model-based approach to investigate the relationship between NIRS measurement results and muscle metabolism.

## ACKNOWLEDGMENT

We are grateful to Hokkaido Red Cross Blood Center for providing blood for performance tests of the developed spatially resolved NIRS instrument.

## REFERENCES

- [1] K. J. Kek, M. Samizo, T. Miyakawa, N. Kudo, and K. Yamamoto, *Proceedings of the 27<sup>th</sup> Annual International Conference of IEEE-EMBS*, Shanghai, China, September 1–4, 2005, Paper 1202, 4.4.2–3 (oral presentation)
- [2] V. Paolo, and M. J. Kushmerick, *Am. J. Physiol. Cell Physiol.*, **279**, C213–224, 2000.
- [3] B. Korzeniewski, and J. A. Zoladz, *Biophys. Chem.*, **92**, pp.17–34, 2001.
- [4] R. A. De Blasi, M. Cope, and M. Ferrari, *Adv. Exp. Med. Biol.*, **317**, pp.771–777, 1992.
- [5] T. Hamaoka *et al.*, *Adv. Exp. Med. Biol.*, **530**, pp.475–483, 2003.
- [6] E. Takahashi and K. Doi, *Jpn. J. Physiol.*, **48**, pp.243–252, 1998.
- [7] R. C. Harris, E. Hultman, and L. O. Nordesjö, *Scand. J. Clin. Lab. Invest.*, **33**, pp.109–120, 1974.
- [8] T. Hamaoka *et al.*, *J. Appl. Physiol.*, **81**(3), pp.1410–1417, 1996.
- [9] J. Karlsson, L. O. Nordesjö, and B. Saltin, *Acta. Physiol. Scand.*, **90**, pp.210–217, 1974.
- [10] M. Saito 1, T. Mano, and S. Iwase, *Eur. J. Appl. Physiol.*, **60**, pp.277–281, 1990.
- [11] R. C. Dennis, and C. R. Valeri, *Clin. Chem.*, **26**(9), pp.1304–1308, 1980.
- [12] P. Moller, and C. Sylven, *Scand. J. Clin. Lab. Invest.*, **41**(5), pp.479–482, 1981.
- [13] R. S. Richardson, E. A. Noyszewski, K. F. Kendrick, J. S. Leigh, and P. D. Wagner, *J. Clin. Invest.*, **96**, pp.1916–1926, 1995.
- [14] M. J. Kushmerick, *Comp. Biochem. Physiol. B*, **96**, pp. 109–123, 1998.

TABLE 1. MAIN PARAMETERS AND CONSTANTS IN THE MATHEMATICAL MODEL OF MUSCLE METABOLISM

Parameter	Definition	Model values	Literature values	Reference
$ATP_o$	ATP concentration in cell water	8.2 mM	8.2 mM	7
$ADP_o$	Initial ADP concentration	18.1 $\mu$ M	18.1 $\mu$ M	8
$PCr_o$	Initial PCr concentration	32 mM	32 mM	8
$Cr_o$	Initial creatine concentration, Cr = Total creatine – PCr	10 mM	10 mM	8
$\dot{V}_{O_{2rest}}$	Resting muscle $O_2$ consumption	1.2 $\mu$ M	1.2 $\mu$ M	8
$Gl_o$	Initial glucose and glycogen concentration	70 mM	65.4–84.4 mM	9
$\dot{Q}_o$	Resting blood flow of the calf muscle	30 mL/(min·L)	30 mL/(min·L)	10
$tHb$	Total hemoglobin concentration,	15 g/dL	14.16 g/dL	11
$tMb$	Total myoglobin concentration,	4.7 mg/g	4.7 mg/g	12
$P_{to}$	$O_2$ partial pressure of capillary	40 mmHg	40 mmHg	13
$P_{vo}$	$O_2$ partial pressure of tissue (estimated value)			Dynamic data